Article

Cell Reports

The Ciliary Margin Zone of the Mammalian Retina Generates Retinal Ganglion Cells

Graphical Abstract

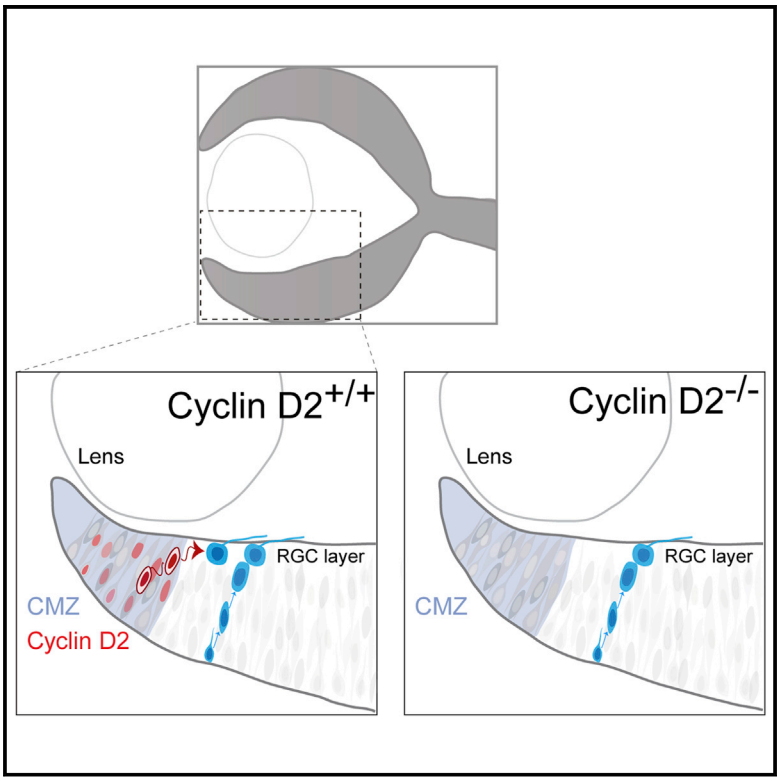

Authors

Florencia Marcucci, Veronica Murcia-Belmonte, Qing Wang, ..., M. Elizabeth Ross, Carol Mason, Eloisa Herrera

Correspondence

e.herrera@umh.es (E.H.), cam4@columbia.edu (C.M.)

In Brief

Is the mammalian CMZ a source of retinal neurons? By live imaging of the mouse retina, Marcucci et al. chronicled cells translocating from the CMZ to the neural retina. In addition, genetic perturbations of CMZ cells implicate the CMZ as a neurogenic site for RGCs.

Highlights

- Live imaging of E14 mouse retina reveals cells moving from the CMZ to the RGC layer
- Cyclin D2 is enriched in the ventral CMZ
- Neurogenesis and RGC numbers are reduced in Cyclin D2$^{-/-}$ neural retina
- Perturbations in the albino CMZ further link the CMZ to RGC production

Marcucci et al., 2016, Cell Reports *17*, 3153–3164
December 20, 2016
http://dx.doi.org/10.1016/j.celrep.2016.11.016

CellPress

Cell Reports
Article

The Ciliary Margin Zone of the Mammalian Retina Generates Retinal Ganglion Cells

Florencia Marcucci,[1,4] Veronica Murcia-Belmonte,[2,4] Qing Wang,[1,5] Yaiza Coca,[2] Susana Ferreiro-Galve,[2] Takaaki Kuwajima,[1] Sania Khalid,[1] M. Elizabeth Ross,[3] Carol Mason,[1,6,*] and Eloisa Herrera[2,*]

[1]Department of Pathology and Cell Biology, College of Physicians and Surgeons, Columbia University, New York, NY 10032, USA
[2]Instituto de Neurociencias de Alicante (Consejo Superior de Investigaciones Científicas-Universidad Miguel Hernández), 03550 Sant Joan d'Alacant, Spain
[3]Center for Neurogenetics, Feil Family Brain & Mind Research Institute, Weill Cornell Medical College, New York, NY 10021, USA
[4]Co-first author
[5]Present address: Department of Ophthalmology, Jules Stein Eye Institute, University of California, Los Angeles, Los Angeles, CA 90095-7000, USA
[6]Lead Contact
*Correspondence: e.herrera@umh.es (E.H.), cam4@columbia.edu (C.M.)
http://dx.doi.org/10.1016/j.celrep.2016.11.016

SUMMARY

The retina of lower vertebrates grows continuously by integrating new neurons generated from progenitors in the ciliary margin zone (CMZ). Whether the mammalian CMZ provides the neural retina with retinal cells is controversial. Live imaging of embryonic retina expressing eGFP in the CMZ shows that cells migrate laterally from the CMZ to the neural retina where differentiated retinal ganglion cells (RGCs) reside. Because Cyclin D2, a cell-cycle regulator, is enriched in ventral CMZ, we analyzed Cyclin D2$^{-/-}$ mice to test whether the CMZ is a source of retinal cells. Neurogenesis is diminished in Cyclin D2 mutants, leading to a reduction of RGCs in the ventral retina. In line with these findings, in the albino retina, the decreased production of ipsilateral RGCs is correlated with fewer Cyclin D2^{+} cells. Together, these results implicate the mammalian CMZ as a neurogenic site that produces RGCs and whose proper generation depends on Cyclin D2 activity.

INTRODUCTION

During development, as the eyecup emerges and expands in size, a wave of neurogenesis progresses from the central retina to the periphery. In fish and amphibians, the distal tip of the retina, referred to as the ciliary marginal zone (CMZ), generates new neurons that are incorporated into the retina as it enlarges continually throughout the lifetime of the animal (Harris and Perron, 1998; Reh and Levine, 1998). In mammals, although the peripheral area of the adult eye is suggested to contain retinal stem cell pools (Ahmad et al., 2000; Coles et al., 2006; Tropepe et al., 2000), its regenerative potential is rather limited. It has in fact been proposed that the mammalian CMZ has independently acquired a mechanism for repressing stem cell division (Tropepe et al., 2000). It is unknown, however, whether the mammalian CMZ is a source of retinal cells during embryogenesis, and whether the loss of neurogenic potential in the CMZ occurs during this period or emerges postnatally.

The CMZ gives rise to two different structures, the iris epithelium and the ciliary body epithelium. In the mouse, these two structures start to differentiate as early as embryonic day 12.5 (E12.5) during the expression of genes such as Msx1 and BMP4, which are detected in the prospective inner ciliary body epithelium but not in the iris epithelium (Zhao et al., 2002; Monaghan et al., 1991). In a recent screen performed in our laboratory, we found that Cyclin D2 is expressed in the CMZ of the mouse retina and is particularly enriched in the ventral retina (Wang et al., 2016). Cyclin D2 is a member of the highly conserved cyclin family and integrates the Cyclin D2-CDK4 complex that phosphorylates and inhibits the retinoblastoma (Rb) protein (Sherr and Roberts, 2004). D-cyclins (D1–D3) regulate cell-cycle progression during G_1/S transition (Kozar and Sicinski, 2005), and although they play similar roles, their function is tissue specific. Cyclin D2 mutant mice show decreased adult neurogenesis in the hippocampus and olfactory bulb, and reduced proliferation of embryonic cortical progenitors (Kowalczyk et al., 2004; Glickstein et al., 2007b, 2009). Moreover, differential expression of Cyclin D2 is associated with the ability to produce distinct neuronal fates (Glickstein et al., 2007a; Petros et al., 2015; Tsunekawa and Osumi, 2012). Neither neurogenesis nor cell fate of Cyclin D2-expressing cells has been examined in the retina.

In the mammalian retina, retinal ganglion cells (RGCs) project to the ipsilateral and contralateral sides of the brain to implement binocular vision. In the mouse, ipsilateral RGCs (iRGCs) reside exclusively in the ventrotemporal (VT) retina, whereas contralateral RGCs (cRGCs) arise from the entire retina. iRGCs express the transcription factor Zic2, the main determinant of the ipsilateral projection (Escalante et al., 2013; Herrera et al., 2003; García-Frigola et al., 2008). In the albino retina, the number of RGCs expressing Zic2 is drastically reduced (Herrera et al., 2003; Bhansali et al., 2014), and it has been proposed that this reduction is the consequence of alterations in retinal neurogenesis (Bhansali et al., 2014; Dräger and Olsen, 1980; Ilia and

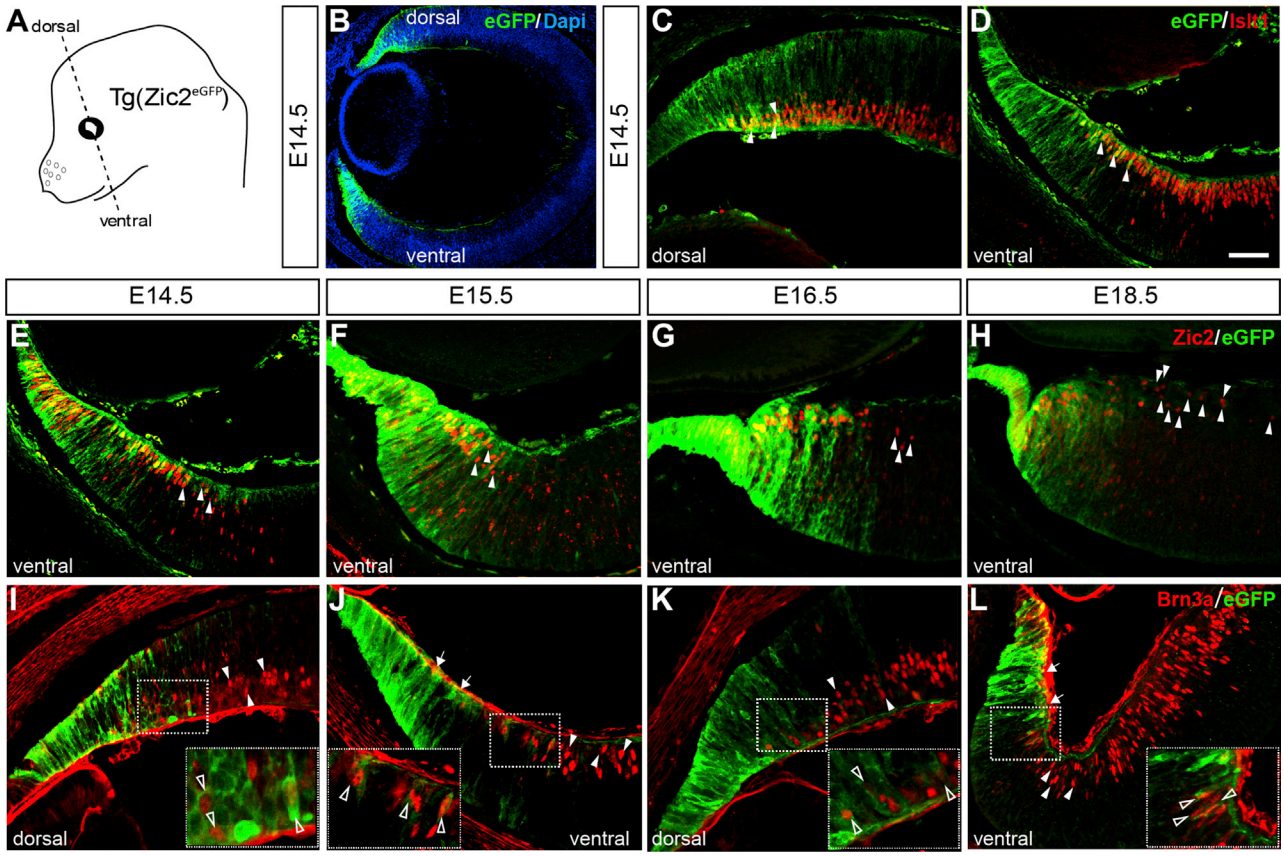

Figure 1. Spatiotemporal Expression of eGFP in the CMZ and Peripheral Neural Retina of Tg(Zic2^{eGFP}) Embryos

(A) Scheme of an embryonic mouse head showing the orientation of coronal sections.

(B) Retinal section of a E14.5 Tg(Zic2^{eGFP}) embryo showing eGFP staining in dorsal and ventral peripheral retina.

(C and D) E14.5 Tg(Zic2^{eGFP}) embryo stained for Islet1 reveals that some RGCs in the peripheral retina express eGFP in both the dorsal (C) and the ventral (D) retina (white arrowheads).

(E–H) Zic2 staining in ventral retinal sections of Tg(Zic2^{eGFP}) embryos at E14.5 (E), E15.5 (F), E16.5 (G), and E18.5 (H) show that eGFP colocalizes with Zic2 in the CMZ and peripheral neural retina but that many Zic2^{+} cells within the peripheral neural retina are not eGFP positive (white arrowheads).

(I–L) Brn3a staining in retinal sections of Tg(Zic2^{eGFP}) embryos at E114.5 (I), E15.5 (F), E16.5 (G), and E18.5 (H) shows that some Brn3a^{+} cells are also eGFP^{+} in both dorsal and ventral retina (open arrowheads), whereas some Brn3a^{+} are eGFP^{-} (white arrowheads). Note the gap of Brn3a^{+} cells in the ventral retina (white arrows in J and L).

Scale bar, 50 μm.

Jeffery, 1996; Rachel et al., 2002; Rice et al., 1995; Webster and Rowe, 1991). However, the link between defects in proliferation in the albino and the reduced number of iRGCs is unclear.

Here, we begin to investigate whether cells destined for the neural retina arise from the CMZ and whether the molecular components of the CMZ including Cyclin D2 relate to the generation of retinal cells. Time-lapse imaging of embryonic retina from a transgenic mouse line that expresses eGFP in CMZ cells indicates that a subpopulation of cells originating in the proximal CMZ moves laterally in addition to radially, to position themselves in the RGC layer. As the proximal ventral CMZ is enriched in Cyclin D2, we asked whether ablation of Cyclin D2 affects the production of retinal cells, specifically RGCs. Consistent with a role for Cyclin D2 in cell-cycle regulation, Cyclin D2$^{-/-}$ mice show decreased proliferation and fewer peripheral RGCs. In addition, albino mice, which have reduced iRGCs, also display fewer Cyclin D2^{+} cells and perturbed proliferation. Together, these results reveal that the CMZ is a source of progenitors giving rise to subpopulations of RGCs in a Cyclin D2-dependent manner.

RESULTS

Zic2 Reporter Mice Express eGFP in the CMZ and Adjacent Neural Retina

We have previously reported that, in the transgenic mouse line Tg(Zic2^{eGFP}), the enhanced fluorescence protein (eGFP) is expressed in the CMZ of embryonic mouse retina (Escalante et al., 2013) (Figure 1), coincident with the expression of the transcription factor Zic2 in this region (Herrera et al., 2003). In this mouse line, eGFP is expressed in some peripheral RGCs located adjacent to the CMZ in both the dorsal and the ventral retina,

confirmed by double immunostaining with Islet1, a general marker for differentiated RGCs (Thor et al., 1991) (Figures 1C and 1D). However, although all iRGCs express the transcription factor Zic2 (Herrera et al., 2003), in this BAC transgenic line, eGFP is expressed only in a subset of iRGCs located at the very periphery of the neural retina, whereas Zic2^{+} cells located more centrally were eGFP^{-} (Figures 1E–1H). In addition, we found that, in both ventral and dorsal retina, some eGFP^{+} cells were also positive for the transcription factor Brn3a (Figures 1I–1L), a marker that labels cRGCs (Quina et al., 2005; Xiang et al., 1995). Together, these observations indicate that, in the Tg(Zic2^{eGFP}) mouse line, even though eGFP does not recapitulate the endogenous expression of Zic2 in iRGCs, some RGCs located at the peripheral neural retina retain eGFP expression, suggesting that they may have an origin in the CMZ.

A Population of Cells Moves Laterally from the CMZ to the Neural Retina

To investigate whether the embryonic CMZ generates neurons that will be incorporated into the peripheral neural retina, we took advantage of the Tg(Zic2^{eGFP}) mouse line to track the behavior of eGFP-labeled cells by time-lapse imaging. By following the movement of eGFP^{+} cells in retinal slices from E14.5 Tg(Zic2^{eGFP}) embryos, we observed a number of cells originally located in the CMZ that moved laterally toward the central retina, ending their trajectories in the zone where differentiated RGCs reside (Figures 2E and 2F).

To better characterize this cellular movement, we analyzed the expression of three CMZ markers: BMP4, Msx1, and Cyclin D2 (Figures 2A–2C and S1). At E14.5–E15.5, Cyclin D2 expression is absent from the BMP4^{+} domain in the most distal CMZ (Figures S1B and S1B′), and this expression coincides with the Msx1^{+} domain (Figures S1C and S1C′). We noted that Msx1 and Cyclin D2 are arrayed in apposing gradients. Msx1 is abundant in the deep (apical) CMZ, whereas Cyclin D2 is enriched in the superficial (basal) CMZ, closer to the vitreous. Based on these expression patterns, we divided the CMZ of the ventral retina into two regions: (1) distal (BMP4^{+}) and (2) proximal (Msx1^{+}/Cyclin D2^{+}) (Figures 2A–2D). In addition, double immunostaining of Cyclin D2 and the RGCs markers Islet1 or Brn3a (Figures S1D–S1G) in retinal sections revealed that Cyclin D2 is restricted to the CMZ and never expressed in differentiated RGCs.

We then categorized the movement of individual eGFP cells by measuring the angle of trajectory (see Experimental Procedures for further details): (1) radial migration, when the trajectory of the eGFP cell followed an angle between 0° and 45°; and (2) lateral migration, when the trajectory of an individual eGFP cell followed an angle greater than 45° from the vertical axis (Figures 2G and 2H). Cell-tracking analysis from the proximal region of the CMZ revealed that 75% of the tracked eGFP cells moved radially following a classic interkinetic apico-basal movement of the nucleus from the deep region of the proximal CMZ to end at the surface of the CMZ (Figure 2I). However, 25% of the tracked cells displayed saltatory movements and translocated in a lateral trajectory, parallel to the surface of the retina, and stopped in a position that corresponds to the RGC layer within the neural retina (Figure 2I). Most of these laterally moving eGFP cells were located in the superficial areas of the proximal CMZ (Figure 2F). We did not find any eGFP cells originally located in the distal (BMP4^{+}) region of the CMZ that displayed a lateral trajectory (Figure 2I).

Notably, and in agreement with the idea that some CMZ cells move laterally toward the neural retina and differentiate into RGCs, we observed eGFP-positive RGC axons in the retina of E16.5 Tg(Zic2^{eGFP}) embryos. These eGFP-labeled axons were visualized to exit the retina through the optic nerve head, at the optic chiasm, and innervate the dorsal lateral geniculate nucleus (dLGN) (Figure S2).

Together, these results suggest that, during embryogenesis, the proximal superficial CMZ of the ventral retina might be a direct source of RGC subsets ultimately destined for the peripheral neural retina.

Mitosis Is Reduced in the CMZ of Cyclin D2-Deficient Mice

Cyclin D2 regulates cell-cycle progression in neural cells and is associated with an intermediate progenitor state in the cortex (Glickstein et al., 2007a, 2009; Tsunekawa et al., 2012). Cyclin D2, but not other members of the Cyclin D family (D1 and D3) (Farhy et al., 2013), is enriched in ventral peripheral retina at early embryonic ages (Wang et al., 2016; Trimarchi et al., 2009) (Figures S1 and S3). Therefore, we decided to investigate the consequences of Cyclin D2 deficiency in retinal cell proliferation by using the mitotic marker PH3 (Figure 3). We compared numbers of PH3^{+} M-phase nuclei in the CMZ and in the neural retina (NR) (boxes in Figures 3A and 3D), in Cyclin D2-deficient (Ccnd2$^{-/-}$; Sicinski et al., 1996) and wild-type (Cyclin D2$^{+/+}$) littermates at E13.5 and E14.5. There were no significant differences in the number of mitotic cells within the neural retina of CyclinD2$^{-/-}$ mice (Figures 3B and 3E). However, fewer cells undergo mitosis in the ventral CMZ of Cyclin D2$^{-/-}$ mice at E13.5 and E14.5 (Figures 3C and 3F). There were no significant differences in the number of PH3^{+} cells in the dorsal CMZ of Cyclin D2$^{-/-}$ mice. This latter observation is not surprising as there are only few Cyclin D2^{+} cells in dorsal retina (Figure S1A). In summary, our results suggest that the absence of Cyclin D2 impairs mitosis in the ventral CMZ.

Neurogenesis of RGCs Is Reduced in Cyclin D2$^{-/-}$ Mice

To further test the possibility that the proximal superficial CMZ is a source of retinal cells, we asked whether ablation of Cyclin D2 affects retinal cell neurogenesis, focusing on the two RGC subtypes that differ by laterality of axonal projection, the ipsilaterally and contralaterally projecting RGCs. Ipsilateral and contralateral RGCs are born at different times during retinal development: cRGCs are generated as early as E10 when they begin to express the markers for differentiated RGCs Islet1 and Brn3b (Rachel et al., 2002). iRGCs are born later, between E13 and E15 (Dräger, 1985; Herrera et al., 2003; F.M. and C.M., unpublished data), and once they are postmitotic, they immediately begin to express Zic2 (Herrera et al., 2003). We performed 5-ethynyl-2′-deoxyuridine (EdU) labeling in Cyclin D2 pregnant dams at E12, E13, and E14, and collected embryos at E15.5 (Figures 4A–4C, S4A, and S4B). To distinguish birthdates of ipsilateral and contralateral RGCs, we counted cells labeled with the following combinations: Zic2^{+}/Islet1^{+}/EdU^{+}

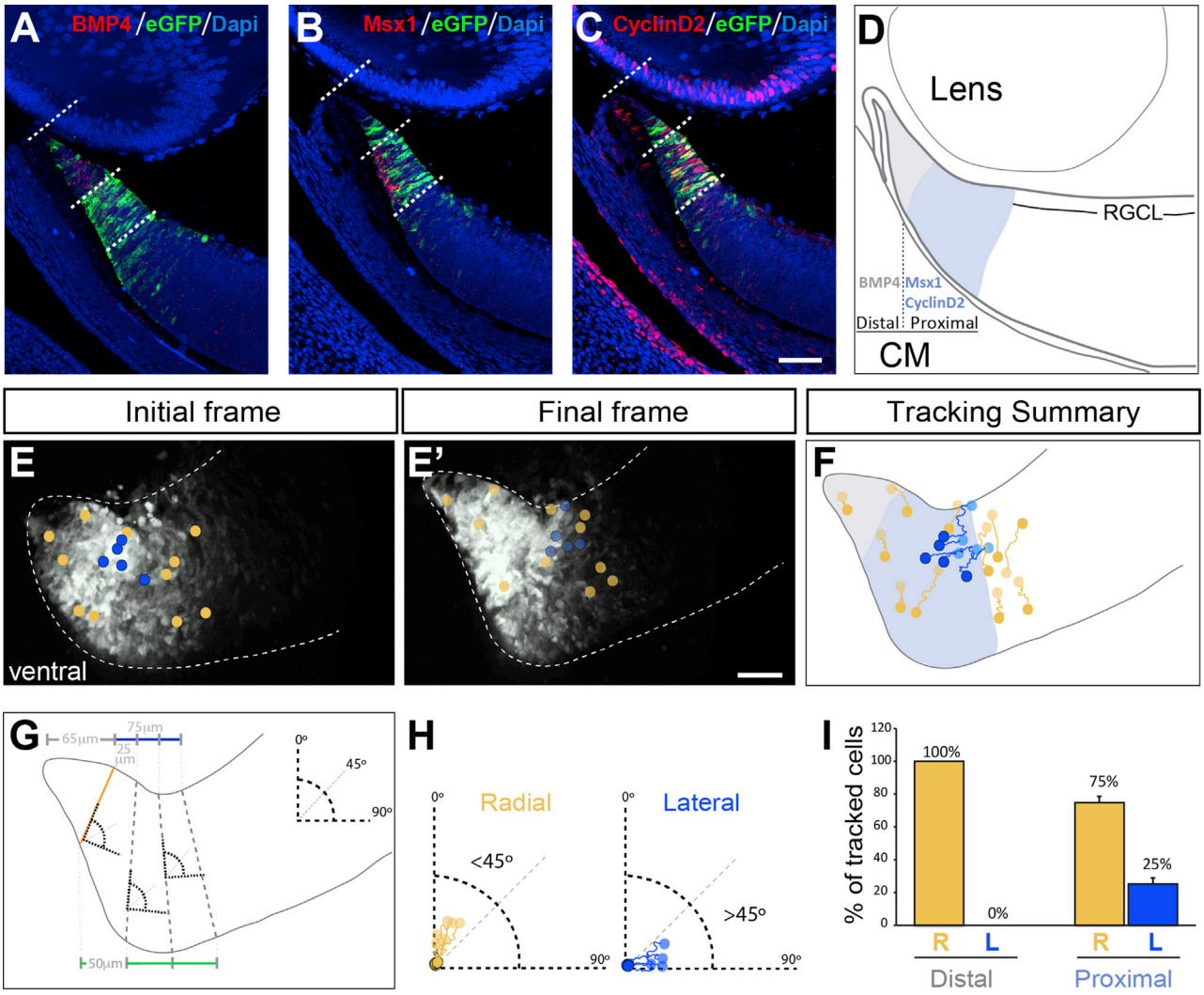

Figure 2. A Population of Cells in the Proximal CMZ at E14.5 Moves Laterally toward the Neural Retina

(A–C) Expression of BMP4, Msx1, and Cyclin D2 in ventral retinal sections at E14.5. BMP4 is expressed in the most distal part of the CMZ, whereas Msx1 and Cyclin D2 label a more proximal region of the CMZ. In addition, Msx1 and Cyclin D2 show complementary patterns of expression along the apico-basal axis of the CMZ: Msx1 is enriched in the most apical (deep) part of the CMZ (B), whereas the majority of Cyclin D2^{+} cells are localized in the basal (superficial) aspect of the CMZ (C).

(D) Schematic drawing summarizing the domains of the CMZ delineated by the expression of BMP4 (gray), Msx1, and Cyclin D2 (blue).

(E and E′) Initial and final frames of a time-lapse sequence from a ventral retinal section of a E14.5 Tg(Zic2^{eGFP}) embryo. Circles in (E) and (E′) indicate the initial and final position of the tracked cells, respectively. Yellow circles indicate cells that follow a radial trajectory and blue circles cells that follow a lateral trajectory (see F–H).

(F) Representative examples of cell trajectories in a retinal section. Note that the majority of the cells showing a lateral trajectory (blue tracings) are located in the basal region of the proximal CMZ (Msx1^{+} region, indicated in blue in the diagram).

(G) Scheme to describe the criteria for categorizing individual cell trackings into radial or lateral trajectories. The CMZ was divided into two regions: the distal (65 μm from the tip) and the proximal region (75 μm toward the central retina) by drawing a line parallel to the retinal surface (gray and blue lines, respectively). A line perpendicular to the surface of the retina (orange line) was defined by the apico-basal columns of progenitors visualized by eGFP staining. The proximal region was divided into three segments by drawing three equidistant lines 25 μm apart at the basal surface of the retina (blue line) and three equidistant lines of 50 μm at the apical surface (green line). Dashed-gray lines limit each segment and were used as a reference where to align 90° angles in each segment.

(H) Individual cell trackings were classified within each segment according to the angles defined in (G). Cells moving in a trajectory with an angle between 0° and 45° from the vertical axis were categorized as radially migrating, and cells with an angle between 45° and 90° were categorized as laterally migrating.

(I) Quantification of radial and lateral trajectories of tracked cells within the distal and the proximal regions of the CMZ. Cells arising from the most distal region of the CMZ display a radial trajectory, whereas a significant number of cells arising from the proximal region of the CMZ move laterally.

Scale bar, 50 μm.

(iRGCs) and Zic2^{-}/Islet1^{+}/EdU^{+} (cRGCs) in VT retina (Figure 4C). From E12 to E14, significantly fewer iRGCs were born in the VT retina of Cyclin D2$^{-/-}$ compared to wild-type littermates (Figure 4C, left panel). However, no difference in the birthdate of Zic2^{-} (cRGCs) was found in VT retina of Cyclin D2$^{-/-}$ at E12–E14 (Figure 4C, right panel).

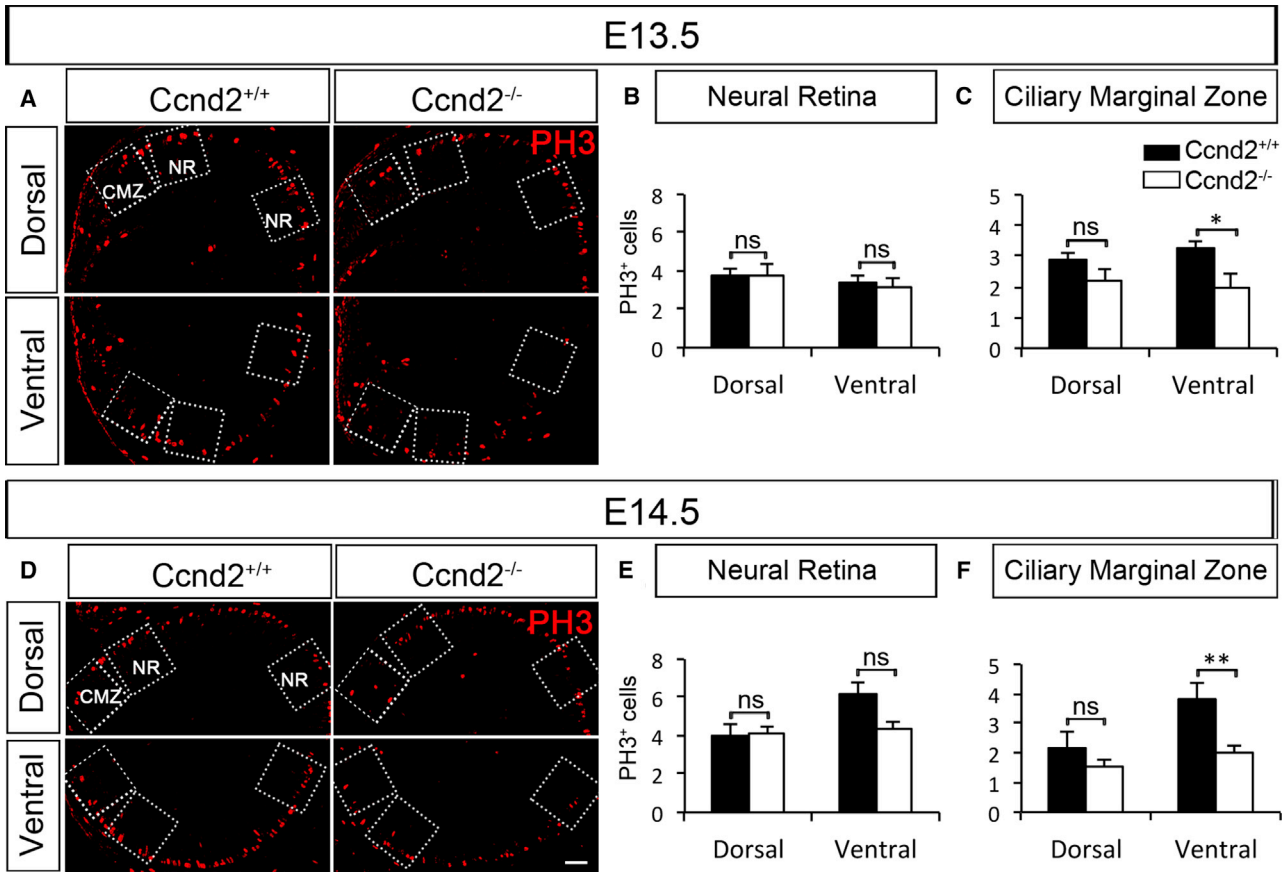

Figure 3. The Mitotic Marker PH3 Shows Reduced Proliferation in Ventral CMZ of Cyclin D2$^{-/-}$ Mice Relative to Wild-Type Littermates

(A and D) Dorsal and ventral retinal sections of Cyclin D2$^{-/-}$ mice and wild-type littermates labeled with the mitotic marker PH3 (red) at E13.5 and E14.5. Quantification of PH3^{+} cells was performed in the retinal regions delineated by the boxed regions in the micrographs; ciliary marginal zone (CMZ) and neural retina (NR).

(B and E) Quantification of PH3^{+} cells in the NR region of ventral and dorsal retina of Cyclin D2$^{-/-}$ and wild-type littermates at E13.5 (B) and E14.5 (E). Although we identified a trend of fewer PH3^{+} cells in the NR region of Cyclin D2$^{-/-}$ mice at E14.5, this difference does not reach significance. Comparable numbers of cells undergo mitosis in the NR region of both dorsal and ventral retina of Cyclin D2$^{-/-}$ mice and wild-type littermates at E13.5 and E14.5.

(C and F) Quantification of PH3^{+} cells in the CMZ region of ventral and dorsal retina of Cyclin D2$^{-/-}$ and wild-type littermates at E13.4 (C) and E14.5 (F). Significantly fewer cells undergo mitosis in the ventral CMZ of Cyclin D2$^{-/-}$ mice compared with wild-type littermates at E13.5 and E14.5. No differences were observed at either age in the corresponding dorsal CMZ.

Student's two-tailed unpaired t test. Error bars represent mean ± SEM. ns, non-significant, $p > 0.05$; *$p < 0.05$; **$p < 0.01$. Scale bar, 40 μm.

Cyclin D2 is first expressed in the VT retina at E11 (Wang et al., 2016). To study whether there are cRGCs dependent on Cyclin D2 that are born at this early stage, we injected EdU at E11 and quantified Brn3a^{+}/Brn3^{+}/EdU^{+} RGCs at E15.5 (Figures 4D–4F) in Cyclin D2$^{-/-}$ and wild-type littermates. We observed a significant reduction in the number of cRGCs born at E11 in VT retina of Cyclin D2$^{-/-}$ mice (Figure 4F). Within dorsotemporal (DT) retina, however, the total number of RGCs and the number of cRGCs born were similar in mutant and wild-type mice (Figures 4F and S4C), indicating that the ablation of Cyclin D2 primarily affects neurogenesis of RGCs that populate VT retina.

Cyclin D2 Is Essential for the Generation of Subpopulations of RGCs

As neurogenesis of iRGCs was consistently reduced during E12–E14 in Cyclin D2$^{-/-}$ retina, we hypothesize that Cyclin D2 in the mouse CMZ houses progenitors that give rise to iRGCs. To test this idea, we quantified the number of RGCs expressing Zic2 (iRGCs) in the ventral retina of Cyclin D2$^{-/-}$ and wild-type littermates during the peak phase of iRGC axonal outgrowth, from E14.5 to E17.5 (Figures 5A and 5B). Although the number of Zic2^{+} RGCs was unaffected at E14.5, E16.5, and E17.5, at E15.5 we observed a 22% reduction in the number of iRGCs in Cyclin D2$^{-/-}$ retina. Importantly, the overall morphology and growth of the retina and lens are not perturbed in the absence of Cyclin D2 (data not shown).

Next, to determine whether the transient reduction of Zic2^{+} RGCs resulted in a diminished ipsilateral projection, we applied DiI crystals monocularly in Cyclin D2$^{-/-}$ and control littermates, and observed 25% fewer ipsilaterally projecting axons in Cyclin D2$^{-/-}$ mice at E17.5 (Figures 5C and 5D). We did not observe stalled axons in the optic nerve or misrouted within

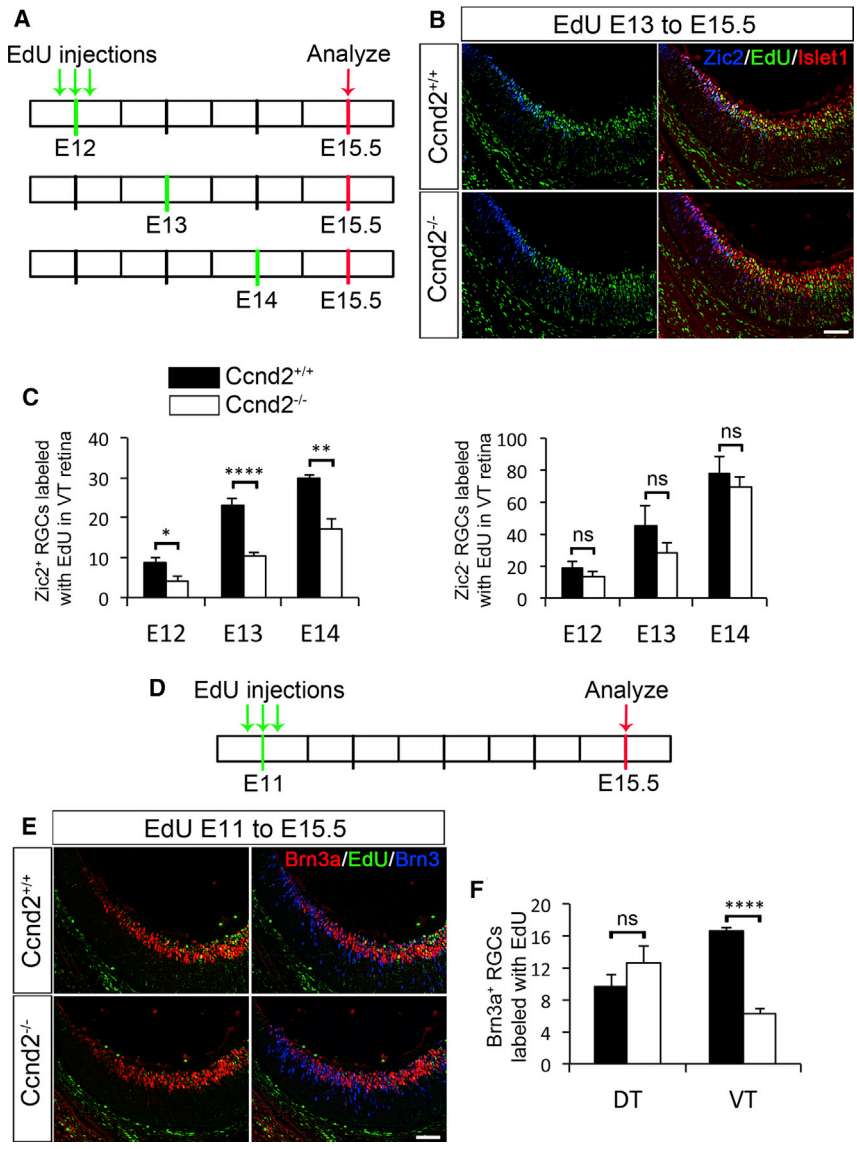

Figure 4. Fewer Ipsilateral RGCs Are Born from E12 to E14 and Fewer Contralateral RGCs Are Born at E11 in VT Retina of Cyclin D2$^{-/-}$ Mice

(A) Time line of EdU birth-dating experiments. Three injections of EdU (10 a.m., 2 p.m., and 6 p.m.) were administered at E12, E13, or E14. Embryos were analyzed at E15.5, the age at which maximum expression of Zic2 is detected.

(B) Representative retinal sections of Cyclin D2$^{-/-}$ and wild-type littermates injected with EdU at E13 to E15.5 and labeled with Zic2 (blue), Islet1 (green), and EdU (green). Representative sections injected with EdU at E12 or E14 can be found in Figure S4.

(C) Left panel: quantification of Zic2$^+$/Islet1$^+$/EdU$^+$ RGCs in VT retina of Cyclin D2$^{-/-}$ and wild-type littermates when EdU was injected at E12, E13, or E14. There is a consistent and significant reduction of ipsilateral RGCs born at E12, E13, and E14 in the Cyclin D2$^{-/-}$ mice when compared to wild-type littermates. Right panel: quantification of Zic2$^-$/Islet1$^+$/EdU$^+$ RGCs in VT retina of Cyclin D2$^{-/-}$ and wild-type littermates. Comparable numbers of contralateral RGCs were born in both genotypes from E12 to E14.

(D) Timeline of EdU injection for birth-date analysis of contralateral RGCs. Three EdU injections were administered at E11, and embryos were analyzed at E15.5.

(E) Retinal sections of Cyclin D2$^{-/-}$ and wild-type littermates injected with EdU at E11 to E15.5 and labeled with Brn3a (red), Brn3 (blue), and EdU (green).

(F) Quantification of Brn3a$^+$/Brn3$^+$/EdU$^+$ RGCs in VT and DT retina of Cyclin D2$^{-/-}$ and wild-type littermates. Fewer contralateral (Brn3a$^+$) RGCs were born at E11 in VT retina of mutant mice. No differences were observed in DT retina of Cyclin D2$^{-/-}$ and wild-type mice.

Student's two-tailed unpaired t test. Error bars represent mean ± SEM. ns, non-significant, $p > 0.05$; *$p < 0.05$; **$p < 0.01$; ****$p < 0.0001$. Scale bar, 40 μm.

the ventral diencephalon, nor within the thalamus (data not shown), suggesting that Cyclin D2 affects the production of iRGCs rather than axon growth and/or guidance.

We also investigated the effect of loss of Cyclin D2 on the output of contralateral cells using Brn3a as a marker (Figures 5E and 5F). At E14.5, we detected a 30% reduction of Brn3a$^+$ RGCs (Figure 5F), and a 19% reduction of the overall number of RGCs (ipsilateral and contralateral RGCs) in VT retina of Cyclin D2$^{-/-}$ mice (Figures 5G and S5A). No differences were observed in the number of Brn3a$^+$ RGCs in DT retina. We did not observe a significant decrease in the number of RGCs expressing Islet2$^+$, a marker expressed by a subset of cRGCs and found in the VT retina after E17 during the later phase of axonal outgrowth (Figure S5B and S5C) (Pak et al., 2004). However, the decrease in the number of cRGCs born at E11 in Cyclin D2$^{-/-}$ retina (Figure 4F) supports the conclusion that Cyclin D2 does contribute to the production of cRGCs generated during early embryogenesis.

Together, these results demonstrate that ablation of Cyclin D2 in the CMZ affects the generation of both ipsilateral and contralateral subtypes of RGCs in the peripheral ventral retina.

The Ventral Retina of Albino Mice Has Fewer Cyclin D2$^+$ Cells and Reduced Proliferation

Albino individuals in all species have a reduced number of iRGCs. This phenotype is associated with mutations in melanin production or melanosome biogenesis and turnover, and leads to decussation defects and mistargeting (Rice et al., 1995; Herrera et al., 2003; Rebsam et al., 2012; Bhansali et al., 2014; Jeffery, 2001). Birth-dating experiments have suggested that this is due to a delay in the generation of RGCs in albino compared with pigmented retina (Bhansali et al., 2014; Dräger, 1985; Giménez

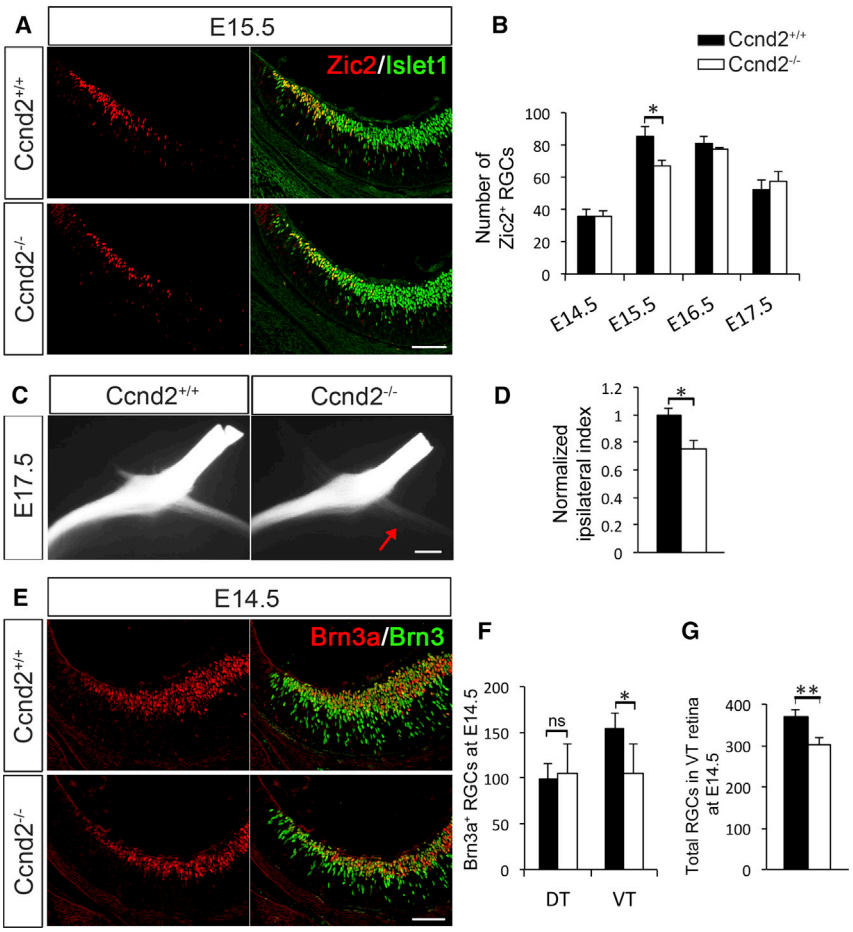

Figure 5. Cyclin D2 Is Necessary for the Generation of Subsets of RGCs

(A) Wild-type and Cyclin D2$^{-/-}$ retinal sections at E15.5 labeled with antibodies against Zic2 (red) and Islet1 (green), indicating ipsilateral and differentiated RGCs, respectively.

(B) Quantification of Zic2^{+}/Islet1^{+} cells in VT retina of Cyclin D2$^{-/-}$ and wild-type littermates at E14.5, E15.5, E16.5, and E17.5. Vertical axis indicates the average number of Zic2^{+}/Islet1^{+} cells per section throughout the ventral retina of Cyclin D2$^{-/-}$ mice and wild-type littermates. The number of ipsilateral RGCs is significantly reduced in Cyclin D2$^{-/-}$ mice at E15.5 but not at the other ages analyzed.

(C) Ventral views of representative whole-mount preparations of Cyclin D2$^{-/-}$ mice and wild-type littermates labeled monocularly with DiI at E17.5. Red arrow indicates fewer ipsilateral axons in the optic tract of the Cyclin D2$^{-/-}$ mouse.

(D) Quantification of the ipsilateral projection through the optic chiasm indicates a significant reduction of ipsilateral axons in Cyclin D2$^{-/-}$ mice at E17.5.

(E) Immunolabeling of wild-type and mutant Cyclin D2 retinal sections with the contralateral RGC marker Brn3a (red) and the pan-RGC marker Brn3 (green) at E14.5.

(F) Quantification of Brn3a^{+}/Brn3^{+} cells shows a significant reduction of cRGCs in VT retina of Cyclin D2$^{-/-}$ mice at E14.5. No significant difference was observed in dorsotemporal (DT) retina.

(G) Quantification of Islet1^{+} cells show a significant reduction in the total number of differentiated RGCs in VT retina of Cyclin D2$^{-/-}$ mice at E14.5.

Student's two-tailed unpaired t test. Error bars represent mean ± SEM. ns, non-significant, $p > 0.05$; *$p \leq 0.05$; **$p \leq 0.01$. Scale bar, 40 μm in (A) and (E); and 200 μm in (C).

et al., 2005; Lavado et al., 2006; Rachel et al., 2002). Given our results suggesting that a number of peripheral RGCs, including 22% of iRGCs, are generated in the CMZ and that their generation depends on Cyclin D2, we asked whether Cyclin D2 expression is compromised in the albino and therefore linked to the reduction of iRGCs. We compared the expression of Cyclin D2 in the retina of pigmented and albino mice at E14.5–E15.5 (Figures 6A and S6A). Whereas Cyclin D2 is highly expressed in the ventral CMZ of pigmented retina, the number of Cyclin D2^{+} cells in the albino retina is significantly reduced, and as in pigmented mice, the Cyclin D2-expressing cells never express Brn3a (Figure S6B). Therefore, the reduction in Cyclin D2^{+} cells in albino ventral retina could be associated with defects in proliferation and thereby with the production of fewer iRGCs.

To test this possibility, we quantified the number of cells positive for the mitotic marker PH3 in the CMZ and the neural retina of pigmented and albino littermates (Figures 6C, 6D, S6C, and S6D). At E14.5, although the number of PH3^{+} cells remains unchanged in the neural retina, the albino ventral CMZ displays a reduced number of mitotic cells when compared to the pigmented CMZ. The reduction in proliferation is restricted to the ventral CMZ, as the numbers of PH3^{+} cells within the dorsal CMZ are comparable in pigmented and albino mice.

Moreover, quantification of the number of Zic2^{+}/eGFP^{+} cells in the neural retina of E16.5 Tg(Zic2^{eGFP}) transgenic embryos in a pigmented or albino background revealed a reduced number of both eGFP^{+} cells and Zic2^{+}/eGFP^{+} cells in the albino (Figure 6B). These data confirm previous reports showing that neurogenesis is altered in the neural retina of albino mice but also indicate that defects in neurogenesis in the albino retina correlate with alterations in the Cyclin D2 population situated in the CMZ.

Together, these results suggest that, during embryogenesis, the proximal superficial CMZ gives rise to subsets of RGCs ultimately located in the peripheral neural retina, and that Cyclin D2 expressed in progenitors of this zone controls the production of RGCs in the VT crescent from which a subset of peripheral RGCs arise.

DISCUSSION

Our study focuses on the CMZ in the embryonic mouse retina and characterizes cell movements and molecular expression in cells of this zone that are associated with the origin of a subpopulation of RGCs. Live imaging of the retina suggests that cells that arise from the proximal superficial aspect of the mouse

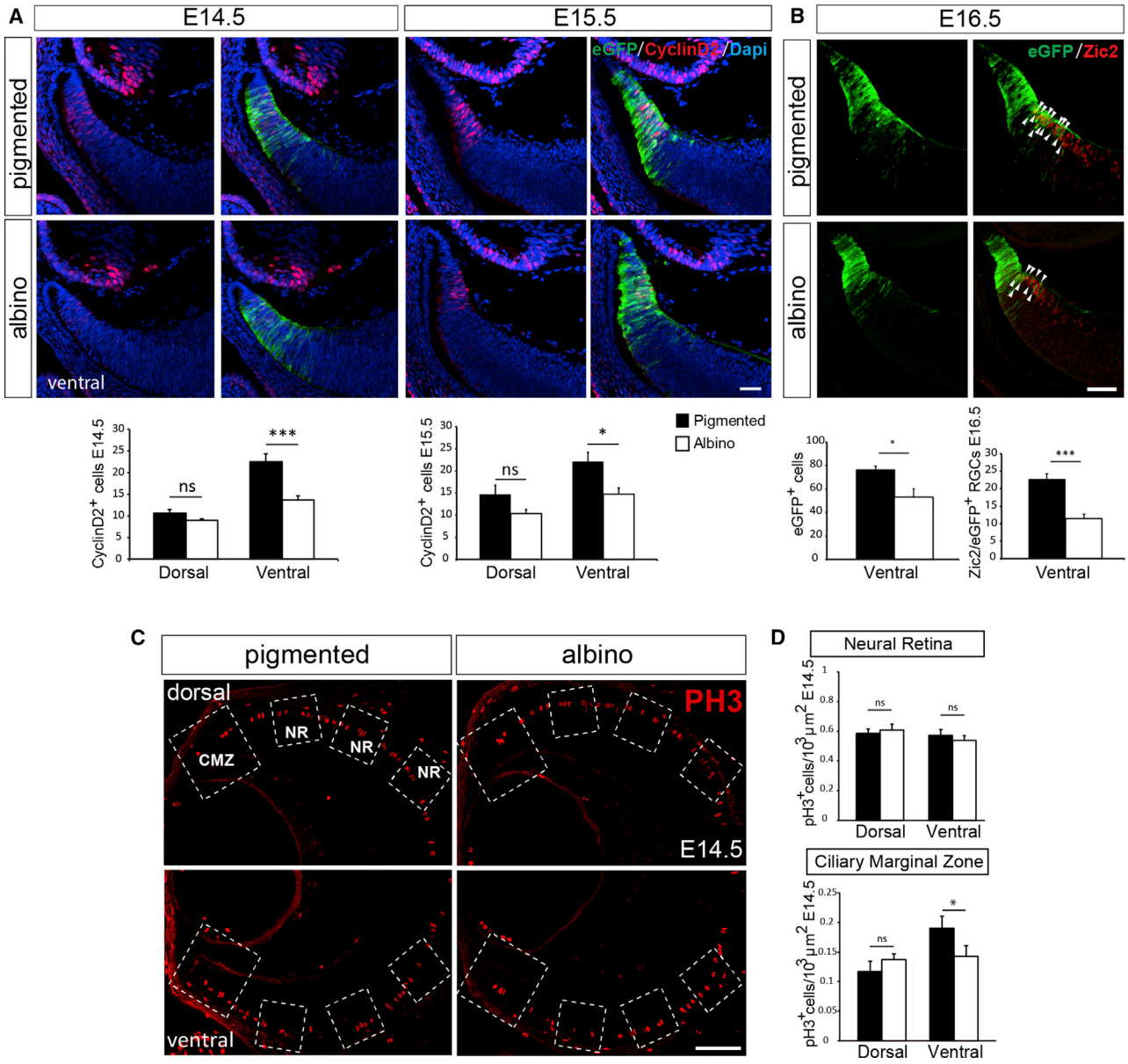

Figure 6. Albino Retinas Have Fewer Cyclin D2$^+$ Cells and Reduced Proliferation When Compared with Pigmented Littermates

(A) Cyclin D2 staining in ventral retinal sections of pigmented and albino littermates at E14.5 and E15.5. Pigmented and albino mice were crossed to Tg(Zic2^{eGFP}) mice to delineate the CMZ by eGFP expression. Quantification of the number of Cyclin D2$^+$ cells in Tg(Zic2^{eGFP}) retinal sections from E14.5 and E15.5 albino retinas compared with their pigmented controls showed a significant reduction in the ventral retina of albino embryos at both E14.5 and E15.5.

(B) Zic2 staining at E16.5 in ventral retinal sections of pigmented and albino littermates crossed to the reporter line Tg(Zic2^{eGFP}). Quantification of the number of Zic2$^+$/eGFP$^+$ cells in E16.5 Tg(Zic2^{eGFP}) retinal sections show a reduction in albino retinas compared with their pigmented controls.

(C) PH3 staining in retinal sections of albinos and pigmented embryos at E14.5. The large square includes the CMZ, whereas the three smaller squares were placed equidistant from each other along the neural retina (NR). Areas inside these squares were used to quantify the number of PH3$^+$ cells in each region.

(D) Quantification of PH3$^+$ cells in the CMZ and the neural retina of E14.5 embryos shows a significant reduction of mitotic cells in the ventral CMZ of albino compared to pigmented embryos.

Student's unpaired t test; error bars represent mean ± SEM. *$p < 0.05$; **$p < 0.01$; ***$p < 0.001$; ns, non-significant. Scale bar, 50 µm.

ventral CMZ translocate laterally toward the adjacent neural retina. In the CMZ, Cyclin D2, a cell-cycle factor regulating cortical proliferation and cell fate choice, is enriched in the ventral CMZ (Figure 7) (Komada et al., 2013; Petros et al., 2015; Tsunekawa et al., 2012; Tsunekawa and Osumi, 2012; Glickstein et al., 2007a, 2009). In the absence of Cyclin D2, mitosis is reduced in the ventral CMZ and fewer ipsilaterally and contralaterally projecting RGCs are generated in the

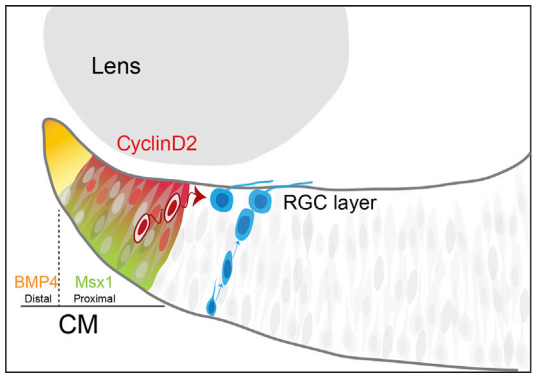

Figure 7. Model of RGCs Neurogenesis in the CMZ

In the CMZ, progenitor cells arise from the Msx1^{+}/Cyclin D2^{+} proximal zone at the periphery of the retina. Two separate and parallel pools of RGC progenitors may co-exist in the retina: one that resides in the deep layers of the neural retina, responsible for the production of the majority of RGCs and where cells divide and migrate radially, and another that resides in the CMZ, whose differentiation into RGCs occurs in a Cyclin D2-dependent manner and from which cells translocate tangentially into the neural retina. Future experiments will determine whether these two proliferative pools are distinct and their respective progeny differ from one other in terms of cell identity and of axonal projection. Overall, these various niches could contribute to cell subtype diversity in the retina.

peripheral retina. Furthermore, in the albino mouse, in which the absence of melanin in the retinal pigment epithelium (RPE) is associated with a reduced production of iRGCs, fewer Cyclin D2^{+} cells are localized in the ventral CMZ and this reduction correlates with a decrease in mitosis. Together, these data support the view that the ventral CMZ gives rise to RGCs in the neural retina in a Cyclin D2-dependent manner.

Mechanism of Cyclin D2 Action

Cyclin Ds are components of the cell-cycle machinery, known to promote Rb phosphorylation and thereby facilitate G_1/S transition. Based on the canonical role of Cyclin D2, and reduced neurogenesis in the CMZ of Cyclin D2$^{-/-}$, we propose a mechanism by which Cyclin D2 could affect cell-cycle progression of a specific subset of CMZ progenitors destined to generate RGCs in the ventral retina. Cyclin D2 has been shown to regulate the length of G_1 and S phases during intermediate progenitor expansion in the embryonic cortex, and in its absence, an increased fraction of progenitors prematurely exit the cell cycle, resulting in reduced proliferation and thus reduced production of cortical neurons (Glickstein et al., 2009). Interestingly, and similar to the Cyclin D2 mutant cortex, the Cyclin D2$^{-/-}$ ventral retina contains fewer mitotic cells and fewer differentiated neurons. In addition, Cyclin D2 mRNA localization in the retinal CMZ is highly reminiscent of the expression of Cyclin D2 in the basal process of cortical neural progenitors where it is believed to maintain progenitors in the cell cycle and thereby influence cell fate (Petros et al., 2015; Trimarchi et al., 2009; Tsunekawa et al., 2012; Tsunekawa and Osumi, 2012; Wang et al., 2016). To determine whether retinal Cyclin D2 acts by changing cell-cycle dynamics, measures of cell-cycle length are needed.

Alternatively, Cyclin D2 could act as a molecular "clock" by regulating the timing or progression of the wave of ventral RGC neurogenesis. A displaced neurogenetic wave is observed in the albino ventral retina, where iRGC production is shifted and, as a consequence, fewer ipsilateral and more contralateral RGCs are born (Bhansali et al., 2014). Indeed, the time of neurogenesis can determine neuronal cell fate and circuitry (Imamura et al., 2011; Molyneaux et al., 2007; Osterhout et al., 2014; Tripodi et al., 2011; Elliott et al., 2008; Mattar et al., 2015; Livesey and Cepko, 2001). Our EdU birth-dating results are in line with the hypothesis that, in the CMZ, CyclinD2 plays a role in cell-cycle regulation within this neurogenic niche. Accordingly, Cyclin D2 marks progenitors in the CMZ that will give rise to a subpopulation of neurons in the neural retina. In the absence of Cyclin D2, the generation of these RGCs is impaired, and the numbers of both ipsilateral and contralateral RGCs are reduced.

Cyclin D2 is necessary to produce both ipsilateral and contralateral RGCs in the peak phase of RGC axonal outgrowth from E14–E17. However, as the number of RGCs that express the cRGC marker Islet2 remains unchanged, it appears that Cyclin D2 is not necessary for the production of cRGCs that express Islet2 and that constitute the late phase of axonal outgrowth within VT retina from E17 until birth (Petros et al., 2008; Pak et al., 2004).

Translocation of Cells from the CMZ to the Neural Retina

Live imaging of retinal slices indicates that, in addition to the expected interkinetic apico-basal nuclei displacement in the peripheral retina, cells in the more proximal and superficial layer of the CMZ were seen to rapidly migrate in the lateral plane, directly into the layer where RGCs are positioned. Future experiments should help to determine whether newly generated cells actively translocate from the CMZ to the neural retina or whether, as it has been observed in zebrafish, they are pushed centrally as a consequence of tissue growth (Wan et al., 2016).

From our experiments, it is unclear whether cells undergoing lateral migration translocate as differentiated cells or as progenitors. We speculate that they become postmitotic once they reach the neural retina, because Islet1 or Brn3, both markers expressed by differentiated RGCs are detected in the neural retina but not in the proximal CMZ.

As we detect eGFP-labeled cells in the dorsal peripheral neural retina of the Tg(Zic2^{eGFP}) mice and as Cyclin D2 is also expressed by a reduced number of cells in the dorsal CMZ (Figure S1), we hypothesize that the lateral movement of CMZ cells is not exclusive to the ventral CMZ. Indeed, during the time-lapse experiments, we observed that a reduced number of dorsal CMZ cells also move laterally (data not shown). In this scenario, the dorsal CMZ would also provide cells to the dorsal neural retina. However, because the number of Brn3a^{+} RGCs in DT retina of Cyclin D2$^{-/-}$ mice was not reduced, we believe that this contribution represents a very small fraction of the total number of differentiated dorsal RGCs.

The Mouse CMZ: A Neurogenic Niche?

The CMZ has been studied as a source of the cells of the iris and ciliary body, and the RPE (Wetts et al., 1989). The retina of fish and amphibians grows continuously throughout life by integrating new cells of the retina arising from proliferating neural progenitors in the CMZ. In these animals, after the initial onset

of neurogenesis in the central retina and as the eye grows in size, new neurons are added from a population of proliferating progenitors located at the CMZ (Perron et al., 1998). In the CMZ of zebrafish, retinal stem cells divide asymmetrically in the radial orientation, allowing the addition of concentric rings of new cells (Wan et al., 2016). The CMZ of the chick is similar to that of fish and amphibians. However, by comparison, most of the avian retina is generated in ovo during early stages of development, and the chick CMZ contributes to the growth of only a small fraction of the retina (Prada et al., 1991; Amato et al., 2004).

Whether the mammalian CMZ displays similar proliferative properties has been long debated (Fischer et al., 2013; Kubota et al., 2002). Retinal stem cells have been identified in the adult mouse CMZ (Tropepe et al., 2000; Ahmad et al., 2000). Moreover, upon genetic injury, the mouse CMZ harbors a population of cells that can proliferate and produce differentiated retinal cells (Moshiri and Reh, 2004; Coles et al., 2006). A recent study identified CMZ-like zones that constitute a source of new retinal progenitor cells in self-organizing retinal cultures derived from human embryonic-derived stem cells (Kuwahara et al., 2015). However, whether the mouse CMZ provides the neural retina with retinal cells under normal conditions in the developing or mature retina has remained elusive.

Here, we show that a subpopulation of differentiated neurons in the neural retina arises through a non-canonical route, from Cyclin D2^{+} progenitors in the CMZ. Our live-imaging studies reveal that cells from the proximal CMZ migrate laterally toward the neural retina. We also show that defects in the generation of CMZ cells in Cyclin D2 mutant mice translate to a reduced production of neural retinal cells in the adjacent retinal compartment. Furthermore, in agreement with our findings, Bélanger et al. (2017) used lineage tracing to demonstrate that both neural and non-neural progeny derive from the embryonic mouse CMZ. Together, both studies suggest that, during embryogenesis, the proximal superficial CMZ could act as a neurogenic area, giving rise to subsets of RGCs ultimately located in the peripheral neural retina.

EXPERIMENTAL PROCEDURES

Mouse Breeding

Mice were housed in a timed-pregnancy breeding colony at Columbia University and at the Instituto de Neurociencias de Alicante, Spain. Conditions and procedures were approved by the Columbia University Institutional Animal Care and Use Committee, protocol numbers AAAG8702 and AAAG9259, and by the Instituto de Neurociencias de Alicante (IN) Animal Care and Use Committee and met European (2013/63/UE) and Spanish regulations (RD 53/2013). In both colonies, females were checked for vaginal plugs at approximately noon each day. E0.5 corresponds to the day when the vaginal plug was detected, with the assumption that conception took place at approximately midnight.

The Tg(Zic2^{EGFP})HT146Gsat line, previously described by Escalante et al. (2013) and Murillo et al. (2015) was obtained from the Mutant Mouse Regional Resource Center. To obtain Tg (Zic2^{EGFP}) pigmented and albino littermates, C57BL/6 Tg (Zic2^{EGFP}) was crossed to Swiss albino mice (CD1/ICR). Cyclin D2-deficient mice, in which exons 1 and 2 have been replaced with a neomycin resistance cassette, were genotyped as originally described (Sicinski et al., 1996) and were shared by the M.E.R. Laboratory.

In Situ Hybridization, Immunohistochemistry, Microscopy, and Analysis of Retinal Sections

In situ hybridization was performed according to reported methods (Schaeren-Wiemers and Gerfin-Moser, 1993) with specific antisense riboprobes for Msx1 (gift of Dr. E.S. Monuki) and Bmp4 (gift of Dr. S. Butler). For immunohistochemistry, antigen retrieval was performed before blocking and incubation with specific primary antibodies. EdU labeling was detected with Click-it reaction after secondary antibody incubation.

For experiments on Tg(Zic2^{eGFP}) and albino tissue, images were captured with an Olympus FV1000 confocal IX81 microscope/FV10-ASW software. For experiments on Cyclin D2 tissue, images were captured with a Zeiss AxioImager M2 microscope equipped with ApoTome, AxioCam MRm camera, and Neurolucida software (version 10.40; MicroBrightField Systems).

Cell numbers were determined by counting the total number of labeled cells in comparable regions of wild-type and mutant coronal retinal sections. Depending on the embryonic stage, two or three sections spanning the rostral to caudal axis were analyzed for a minimum of three animals per age and genotype.

Video Time-Lapse Tracking of Cell Migration

Images for the video time-lapse (VTL) tracking were taken every 20 min over 20 hr, with a laser-scanning spectral confocal microscope (TCS SP2; Leica) with long working distance and water-immersion 20× objective. To track cell trajectories, we used IMARIS Surpass software as it allows the visualization of each cell in 3D. To subtract the cellular movements due to the physiological tissue growth during image acquisition from the active lateral movements of the cells, we applied the ImageJ plugin "Correct 3D drift" before cell tracking (Parslow et al., 2014). To determine whether cells underwent a radial or lateral path, a straight line between the start and the end point of each cell trajectory was drawn (trajectory straight line [TSL]). In the final frame of each movie, the CMZ was divided into two regions: the distal region (65 μm from the tip) and the proximal region (75 μm to the central retina) by drawing a line parallel to the retinal surface (gray and blue lines, respectively, in Figure 2G). A line perpendicular to the surface of the retina was delineated (orange line) following the natural shape of the apico-basal progenitors easily visualized by eGFP staining. The proximal region was then divided into three subregions by drawing three equidistant lines separated 25 μm in the basal surface (blue line) and 50 μm in the apical surface (green line). To define the angle of the trajectory of each cell, the TSL was aligned to the nearest reference line located to the left of the cell trajectory starting point and classified as greater or less than 45°. Six independent cell-tracking experiments were carried out for each genotype, and at least 15 cells were analyzed in each experiment.

Anterograde Labeling of Retinal Axons with DiI

Anterograde whole-eye DiI labeling was performed to E17 embryonic heads fixed in 4% PFA ON by implanting DiI crystals unilaterally into the optic disc. Heads were incubated in PBS containing 0.1% sodium azide for 5–7 days at 37°C. Specimens were photographed as whole mounts on a Leica DFC365 FX fluorescence stereo microscope with digital camera. For quantification of the ipsilateral projection, pixel intensity of DiI^{+} ipsilateral and contralateral optic tracts adjacent to chiasm midline in a 500 × 500-μm area was measured with ImageJ analysis software. The ipsilateral index was obtained by dividing the intensity of the ipsilateral projection as seen in whole mounts by the sum of the contralateral and ipsilateral pixel intensities. Each of the ipsilateral indexes in mutants was normalized to the WT ipsilateral index.

Statistical Analysis

All data were analyzed and graphs constructed using Microsoft Excel. All error bars are expressed as the SEM. Statistical significance was determined using two-tailed unpaired Student's t test. ns, non-significant, $p > 0.05$; *$p \leq 0.05$; **$p \leq 0.01$; ***$p \leq 0.001$; ****$p \leq 0.0001$.

For further details, please refer to Supplemental Experimental Procedures.

SUPPLEMENTAL INFORMATION

Supplemental Information includes Supplemental Experimental Procedures, six figures, and one movie and can be found with this article online at http://dx.doi.org/10.1016/j.celrep.2016.11.016.

AUTHOR CONTRIBUTIONS

F.M. designed, performed, and analyzed the experiments shown in Figures 3, 4, 5, and S3–S5, and, together with E.H., wrote and revised the manuscript. V.M.-B. designed, performed, and analyzed experiments shown in Figures 1, 2, 6, 7, S1, S2, and S6, and revised the manuscript. Q.W. first identified Cyclin D2 enrichment in ventral retina, designed and performed pilot experiments on the Cyclin D2 mutant, and commented on the manuscript. Y.C. optimized the conditions for time-lapse experiments and assisted in live imaging. S.F.-G. characterized the Tg(Zic2GFP) mice shown in Figures 1A–1H. T.K. performed and quantified axon tracing in Figures 5C and 5D. S.K. helped in cell counting in Figure 5. M.E.R. provided the Cyclin D2 mice, provided critical discussions of experiments involving Cyclin D2, and commented on the manuscript. E.H. wrote the original draft, and C.M. and E.H. (co-corresponding authors) revised subsequent versions of the manuscript, conceived and supervised the study, and secured funding in their respective laboratories.

ACKNOWLEDGMENTS

We thank Dr. Peter Sicinski for sharing the Cyclin D2 mice through the M.E.R. laboratory, Corinne Quirk for assistance with cell counting, Mika Melikyan for mouse breeding and genotyping, Giovanna Expósito for assistance with microscopy analysis, and Jane Dodd and members of the C.M. and E.H. laboratory for discussion and comments on the manuscript. This paper was supported by NIH grants R01 EY012736 and EY015290 (C.M.), T32 GM07367 and EY013933 (Q.W.), and P01 NS 048120 (M.E.R.), Fight for Sight (F.M.), PROMETEO 2012/026 (Valencia Regional Government), BFU2016-77605 (Spanish Government), PCIN2015-192-C02-02 (ERA-Net), 20142130 (Marató-TV3 Foundation), 201/C/2014 (Tatiana Pérez de Guzmán el Bueno Foundation), and European Research Council (no. 282329; E.H.). The Instituto de Neurociencias is a Severo Ochoa Excellence Center (SEV-2013-0317).

Received: June 17, 2016
Revised: September 23, 2016
Accepted: November 1, 2016
Published: December 20, 2016

REFERENCES

Ahmad, I., Tang, L., and Pham, H. (2000). Identification of neural progenitors in the adult mammalian eye. Biochem. Biophys. Res. Commun. *270*, 517–521.

Amato, M.A., Arnault, E., and Perron, M. (2004). Retinal stem cells in vertebrates: parallels and divergences. Int. J. Dev. Biol. *48*, 993–1001.

Bhansali, P., Rayport, I., Rebsam, A., and Mason, C. (2014). Delayed neurogenesis leads to altered specification of ventrotemporal retinal ganglion cells in albino mice. Neural Dev. *9*, 11.

Bélanger, M.-C., Robert, B., and Cayouette, M. (2017). Msx1-positive progenitors in the retinal ciliary margin give rise to both neural and non-neural progenies in mammals. Dev. Cell. *40*, Published online December 20, 2016. http://dx.doi.org/10.1016/j.devcel.2016.11.020.

Coles, B.L., Horsford, D.J., McInnes, R.R., and van der Kooy, D. (2006). Loss of retinal progenitor cells leads to an increase in the retinal stem cell population in vivo. Eur. J. Neurosci. *23*, 75–82.

Dräger, U.C. (1985). Birth dates of retinal ganglion cells giving rise to the crossed and uncrossed optic projections in the mouse. Proc. R. Soc. Lond. B Biol. Sci. *224*, 57–77.

Dräger, U.C., and Olsen, J.F. (1980). Origins of crossed and uncrossed retinal projections in pigmented and albino mice. J. Comp. Neurol. *191*, 383–412.

Elliott, J., Jolicoeur, C., Ramamurthy, V., and Cayouette, M. (2008). Ikaros confers early temporal competence to mouse retinal progenitor cells. Neuron *60*, 26–39.

Escalante, A., Murillo, B., Morenilla-Palao, C., Klar, A., and Herrera, E. (2013). Zic2-dependent axon midline avoidance controls the formation of major ipsilateral tracts in the CNS. Neuron *80*, 1392–1406.

Farhy, C., Elgart, M., Shapira, Z., Oron-Karni, V., Yaron, O., Menuchin, Y., Rechavi, G., and Ashery-Padan, R. (2013). Pax6 is required for normal cell-cycle exit and the differentiation kinetics of retinal progenitor cells. PLoS One *8*, e76489.

Fischer, A.J., Bosse, J.L., and El-Hodiri, H.M. (2013). The ciliary marginal zone (CMZ) in development and regeneration of the vertebrate eye. Exp. Eye Res. *116*, 199–204.

García-Frigola, C., Carreres, M.I., Vegar, C., Mason, C., and Herrera, E. (2008). Zic2 promotes axonal divergence at the optic chiasm midline by EphB1-dependent and -independent mechanisms. Development *135*, 1833–1841.

Giménez, E., Lavado, A., Jeffery, G., and Montoliu, L. (2005). Regional abnormalities in retinal development are associated with local ocular hypopigmentation. J. Comp. Neurol. *485*, 338–347.

Glickstein, S.B., Alexander, S., and Ross, M.E. (2007a). Differences in cyclin D2 and D1 protein expression distinguish forebrain progenitor subsets. Cereb. Cortex *17*, 632–642.

Glickstein, S.B., Moore, H., Slowinska, B., Racchumi, J., Suh, M., Chuhma, N., and Ross, M.E. (2007b). Selective cortical interneuron and GABA deficits in cyclin D2-null mice. Development *134*, 4083–4093.

Glickstein, S.B., Monaghan, J.A., Koeller, H.B., Jones, T.K., and Ross, M.E. (2009). Cyclin D2 is critical for intermediate progenitor cell proliferation in the embryonic cortex. J. Neurosci. *29*, 9614–9624.

Harris, W.A., and Perron, M. (1998). Molecular recapitulation: the growth of the vertebrate retina. Int. J. Dev. Biol. *42*, 299–304.

Herrera, E., Brown, L., Aruga, J., Rachel, R.A., Dolen, G., Mikoshiba, K., Brown, S., and Mason, C.A. (2003). Zic2 patterns binocular vision by specifying the uncrossed retinal projection. Cell *114*, 545–557.

Ilia, M., and Jeffery, G. (1996). Delayed neurogenesis in the albino retina: evidence of a role for melanin in regulating the pace of cell generation. Brain Res. Dev. Brain Res. *95*, 176–183.

Imamura, F., Ayoub, A.E., Rakic, P., and Greer, C.A. (2011). Timing of neurogenesis is a determinant of olfactory circuitry. Nat. Neurosci. *14*, 331–337.

Jeffery, G. (2001). Architecture of the optic chiasm and the mechanisms that sculpt its development. Physiol. Rev. *81*, 1393–1414.

Komada, M., Iguchi, T., Takeda, T., Ishibashi, M., and Sato, M. (2013). Smoothened controls cyclin D2 expression and regulates the generation of intermediate progenitors in the developing cortex. Neurosci. Lett. *547*, 87–91.

Kowalczyk, A., Filipkowski, R.K., Rylski, M., Wilczynski, G.M., Konopacki, F.A., Jaworski, J., Ciemerych, M.A., Sicinski, P., and Kaczmarek, L. (2004). The critical role of cyclin D2 in adult neurogenesis. J. Cell Biol. *167*, 209–213.

Kozar, K., and Sicinski, P. (2005). Cell cycle progression without cyclin D-CDK4 and cyclin D-CDK6 complexes. Cell Cycle *4*, 388–391.

Kubota, R., Hokoc, J.N., Moshiri, A., McGuire, C., and Reh, T.A. (2002). A comparative study of neurogenesis in the retinal ciliary marginal zone of homeothermic vertebrates. Brain Res. Dev. Brain Res. *134*, 31–41.

Kuwahara, A., Ozone, C., Nakano, T., Saito, K., Eiraku, M., and Sasai, Y. (2015). Generation of a ciliary margin-like stem cell niche from self-organizing human retinal tissue. Nat. Commun. *6*, 6286.

Lavado, A., Jeffery, G., Tovar, V., de la Villa, P., and Montoliu, L. (2006). Ectopic expression of tyrosine hydroxylase in the pigmented epithelium rescues the retinal abnormalities and visual function common in albinos in the absence of melanin. J. Neurochem. *96*, 1201–1211.

Livesey, F.J., and Cepko, C.L. (2001). Vertebrate neural cell-fate determination: lessons from the retina. Nat. Rev. Neurosci. *2*, 109–118.

Mattar, P., Ericson, J., Blackshaw, S., and Cayouette, M. (2015). A conserved regulatory logic controls temporal identity in mouse neural progenitors. Neuron *85*, 497–504.

Molyneaux, B.J., Arlotta, P., Menezes, J.R., and Macklis, J.D. (2007). Neuronal subtype specification in the cerebral cortex. Nat. Rev. Neurosci. *8*, 427–437.

Monaghan, A.P., Davidson, D.R., Sime, C., Graham, E., Baldock, R., Bhattacharya, S.S., and Hill, R.E. (1991). The Msh-like homeobox genes define domains in the developing vertebrate eye. Development *112*, 1053–1061.

Moshiri, A., and Reh, T.A. (2004). Persistent progenitors at the retinal margin of ptc$^{+/-}$ mice. J. Neurosci. *24*, 229–237.

Murillo, B., Ruiz-Reig, N., Herrera, M., Fairén, A., and Herrera, E. (2015). Zic2 controls the migration of specific neuronal populations in the developing forebrain. J. Neurosci. *35*, 11266–11280.

Osterhout, J.A., El-Danaf, R.N., Nguyen, P.L., and Huberman, A.D. (2014). Birthdate and outgrowth timing predict cellular mechanisms of axon target matching in the developing visual pathway. Cell Rep. *8*, 1006–1017.

Pak, W., Hindges, R., Lim, Y.S., Pfaff, S.L., and O'Leary, D.D. (2004). Magnitude of binocular vision controlled by islet-2 repression of a genetic program that specifies laterality of retinal axon pathfinding. Cell *119*, 567–578.

Parslow, A., Cardona, A., and Bryson-Richardson, R.J. (2014). Sample drift correction following 4D confocal time-lapse imaging. J. Vis. Exp. *86*, 51086.

Perron, M., Kanekar, S., Vetter, M.L., and Harris, W.A. (1998). The genetic sequence of retinal development in the ciliary margin of the Xenopus eye. Dev. Biol. *199*, 185–200.

Petros, T.J., Rebsam, A., and Mason, C.A. (2008). Retinal axon growth at the optic chiasm: to cross or not to cross. Annu. Rev. Neurosci. *31*, 295–315.

Petros, T.J., Bultje, R.S., Ross, M.E., Fishell, G., and Anderson, S.A. (2015). Apical versus basal neurogenesis directs cortical interneuron subclass fate. Cell Rep. *13*, 1090–1095.

Prada, C., Puga, J., Pérez-Méndez, L., López And, R., and Ramírez, G. (1991). Spatial and temporal patterns of neurogenesis in the chick retina. Eur. J. Neurosci. *3*, 1187.

Quina, L.A., Pak, W., Lanier, J., Banwait, P., Gratwick, K., Liu, Y., Velasquez, T., O'Leary, D.D., Goulding, M., and Turner, E.E. (2005). Brn3a-expressing retinal ganglion cells project specifically to thalamocortical and collicular visual pathways. J. Neurosci. *25*, 11595–11604.

Rachel, R.A., Dolen, G., Hayes, N.L., Lu, A., Erskine, L., Nowakowski, R.S., and Mason, C.A. (2002). Spatiotemporal features of early neuronogenesis differ in wild-type and albino mouse retina. J. Neurosci. *22*, 4249–4263.

Rebsam, A., Bhansali, P., and Mason, C.A. (2012). Eye-specific projections of retinogeniculate axons are altered in albino mice. J. Neurosci. *32*, 4821–4826.

Reh, T.A., and Levine, E.M. (1998). Multipotential stem cells and progenitors in the vertebrate retina. J. Neurobiol. *36*, 206–220.

Rice, D.S., Williams, R.W., and Goldowitz, D. (1995). Genetic control of retinal projections in inbred strains of albino mice. J. Comp. Neurol. *354*, 459–469.

Schaeren-Wiemers, N., and Gerfin-Moser, A. (1993). A single protocol to detect transcripts of various types and expression levels in neural tissue and cultured cells: in situ hybridization using digoxigenin-labelled cRNA probes. Histochemistry *100*, 431–440.

Sherr, C.J., and Roberts, J.M. (2004). Living with or without cyclins and cyclin-dependent kinases. Genes Dev. *18*, 2699–2711.

Sicinski, P., Donaher, J.L., Geng, Y., Parker, S.B., Gardner, H., Park, M.Y., Robker, R.L., Richards, J.S., McGinnis, L.K., Biggers, J.D., et al. (1996). Cyclin D2 is an FSH-responsive gene involved in gonadal cell proliferation and oncogenesis. Nature *384*, 470–474.

Thor, S., Ericson, J., Brännström, T., and Edlund, T. (1991). The homeodomain LIM protein Isl-1 is expressed in subsets of neurons and endocrine cells in the adult rat. Neuron *7*, 881–889.

Trimarchi, J.M., Cho, S.H., and Cepko, C.L. (2009). Identification of genes expressed preferentially in the developing peripheral margin of the optic cup. Dev. Dyn. *238*, 2327–2329.

Tripodi, M., Stepien, A.E., and Arber, S. (2011). Motor antagonism exposed by spatial segregation and timing of neurogenesis. Nature *479*, 61–66.

Tropepe, V., Coles, B.L., Chiasson, B.J., Horsford, D.J., Elia, A.J., McInnes, R.R., and van der Kooy, D. (2000). Retinal stem cells in the adult mammalian eye. Science *287*, 2032–2036.

Tsunekawa, Y., and Osumi, N. (2012). How to keep proliferative neural stem/progenitor cells: a critical role of asymmetric inheritance of cyclin D2. Cell Cycle *11*, 3550–3554.

Tsunekawa, Y., Britto, J.M., Takahashi, M., Polleux, F., Tan, S.S., and Osumi, N. (2012). Cyclin D2 in the basal process of neural progenitors is linked to non-equivalent cell fates. EMBO J. *31*, 1879–1892.

Wan, Y., Almeida, A.D., Rulands, S., Chalour, N., Muresan, L., Wu, Y., Simons, B.D., He, J., and Harris, W.A. (2016). The ciliary marginal zone of the zebrafish retina: clonal and time-lapse analysis of a continuously growing tissue. Development *143*, 1099–1107.

Wang, Q., Marcucci, F., Cerullo, I., and Mason, C. (2016). Ipsilateral and contralateral retinal ganglion cells express distinct genes during decussation at the optic chiasm. eNeuro. Published online November 17, 2016. http://dx.doi.org/10.1523/ENEURO.0169-16.2016.

Webster, M.J., and Rowe, M.H. (1991). Disruption of developmental timing in the albino rat retina. J. Comp. Neurol. *307*, 460–474.

Wetts, R., Serbedzija, G.N., and Fraser, S.E. (1989). Cell lineage analysis reveals multipotent precursors in the ciliary margin of the frog retina. Dev. Biol. *136*, 254–263.

Xiang, M., Zhou, L., Macke, J.P., Yoshioka, T., Hendry, S.H., Eddy, R.L., Shows, T.B., and Nathans, J. (1995). The Brn-3 family of POU-domain factors: primary structure, binding specificity, and expression in subsets of retinal ganglion cells and somatosensory neurons. J. Neurosci. *15*, 4762–4785.

Zhao, S., Chen, Q., Hung, F.C., and Overbeek, P.A. (2002). BMP signaling is required for development of the ciliary body. Development *129*, 4435–4442.